Vulnerability Functions for RC Shear Wall Buildings in Australia

Ryan Hoult,[a),] Helen Goldsworthy,[a)] and Elisa Lumantarna[a)]

This research investigates the vulnerability of the reinforced concrete shear wall building stock of Australia by conducting an assessment of these types of structures in the city of Melbourne. The assessment uses the best information available for selecting the building parameters applicable to the low-to-moderate seismic region, site soil class, expected earthquake ground motions and site response. The capacity spectrum method is used to derive vulnerability functions for low-rise, mid-rise and high-rise reinforced concrete shear wall buildings. Comparisons are made to other estimates, which show that the results derived from the research here indicate a more vulnerable reinforced concrete shear wall building stock.

INTRODUCTION

Vulnerability (or fragility) functions are useful for risk assessments, used by insurance companies and implemented in loss estimation software such as EQRM (Robinson *et al.*, 2005) from Geoscience Australia. EQRM uses the methodology based on HAZUS (FEMA, 2010), which typically use generic building parameters to estimate the capacity of a structure. However, building and construction codes of practice internationally can differ quite significantly in comparison to the Australian Standards, particularly with seismically active regions and the United States where the HAZUS (FEMA, 2010) methodology is utilized. This might not make it viable for loss methodology and risk assessments carried out in Australia, a low-to-moderate seismic region, to adopt other models and values of capacity parameters, such as those from HAZUS (FEMA, 2010), that have been developed in regions where the building codes differ significantly. This is also discussed in Edwards *et al*. (2004), where the authors revised some of the parameters from HAZUS to better reflect the Australian building stock using the available damage distribution data caused by the Newcastle earthquake in 1989. Edwards *et al*. (2004) found that the United States building stock tended to be 'much less vulnerable than the corresponding Australian construction'.

[a)] University of Melbourne, Department of Infrastructure Engineering, Parkville, VIC, 3010, Australia

However, these parameters were only revised for typical residential structures, whereas the focus of this research is commercial and residential reinforced concrete (RC) shear wall buildings. Although HAZUS (FEMA, 2003) have building parameters for "Pre-Code" buildings, which correspond to structures that have not been seismically designed, it is possible that the findings from Edwards *et al*. (2004) will also hold true for the comparisons made from the fragility curves derived from generic building parameters provided by HAZUS (FEMA, 2003) to that derived from an extensive number of capacity curves which better reflect the RC structural wall building stock in Australia. This is primarily because of the poor performance observed from lightly reinforced and unconfined concrete walls in recent earthquake events (Beca, 2011; CERC, 2012; Henry, 2013; Morris *et al.*, 2015; Sritharan *et al.*, 2014; Wallace *et al.*, 2012). Due to the low standard of detailing required in the current materials standards in Australia, and the low earthquake return period typically used in design, it is anticipated that most of the RC walls and cores embedded within structures around Australia are lightly reinforced and unconfined and this is likely to lead to brittle behavior in an earthquake.

This research focuses on deriving vulnerability (or fragility) functions for RC shear wall buildings in Australia using the capacity spectrum method (CSM) to assess a large variability of buildings that are commonly found in the low-to-moderate seismic region.

METHODOLOGY

A flow chart of the proposed assessment program to be written in MATLAB (Ingle & Proakis, 2016) is presented in Figure 1. The following sections discuss the individual components of the assessment program to derive the vulnerability functions. The consequence of these results are discussed at a later stage of the paper, where some comparisons are made to vulnerability functions that are currently thought to be representative of the RC building stock of Australia.

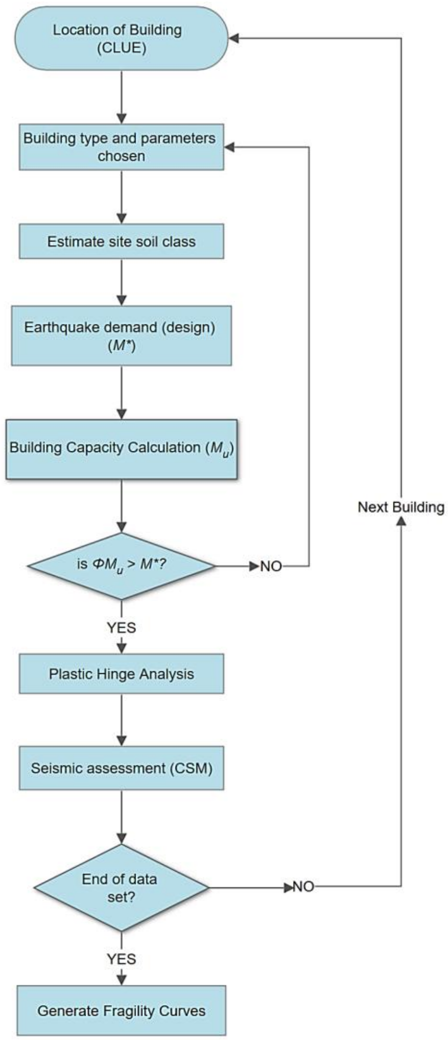

Figure 1 Flow chart of the program to derive seismic fragility curves

CLUE BUILDING INVENTORY

The Census of Land Use and Employment (CLUE) dataset (Melbourne City Council, 2015) is a valuable research tool providing comprehensive information, including:

- Construction year
- Number of floors (above ground)
- Building material

- Location (latitude and longitudinal coordinates)
- Gross floor area

The total number of LR ($2 \leq n \leq 3$), MR ($4 \leq n \leq 7$) and HR ($8 \leq n \leq 12$) "concrete" buildings that will be used from the CLUE dataset for the seismic assessment is 821, 363 and 219 respectively, where n is the number of storeys. The definition of the low-rise, mid-rise and high-rise, corresponding to the number of storeys, has been adopted from FEMA (2010). This definition has also been adopted in EQRM (Robinson *et al.*, 2005) and GAR15 (Maqsood *et al.*, 2014). It should also be emphasized that the HR buildings investigated here have a 12-storey limit as buildings taller than this are likely to have higher mode effects not captured by the capacity spectrum method (Mehdipanah *et al.*, 2016). It is assumed that these buildings are RC shear wall structures that can be idealized with the building types presented in the next section (shown in Figure 3). The total number of buildings are also mapped with their corresponding location given in Figure 2.

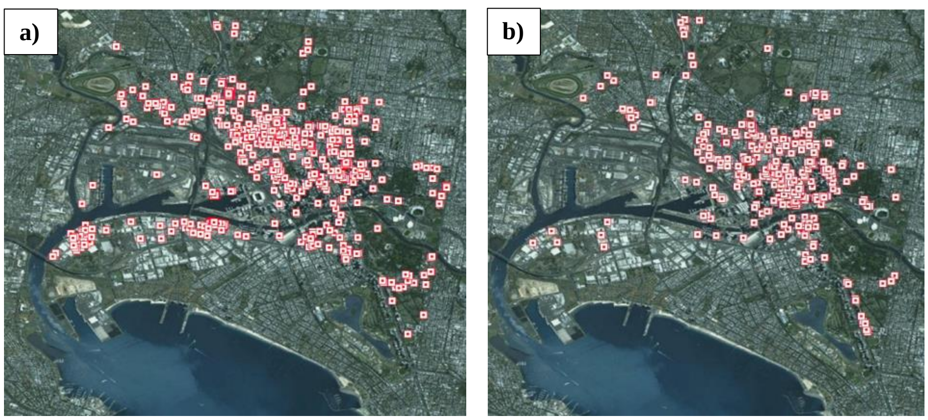

Figure 2 Location of (a) LR (b) MR and (c) HR buildings used from the CLUE dataset

The extensive information provided by CLUE (Melbourne City Council, 2015) on concrete buildings in Melbourne provides crucial information that will ultimately be used to derive the initial design base shear for the individual structures. The building parameters and corresponding values that will be used in the MATLAB assessment program are discussed in the next Section.

BUILDING VARIABILITY

Different Building Types, varying by the use of rectangular and/or C-shaped RC walls for the lateral load resisting elements, are to be used in representing the idealized buildings for Australia. Other researchers have followed similar methods in idealizing the RC building stock for seismic performance studies (Hancock & Bommer, 2007; Lestuzzi & Bachmann, 2007; Mwafy & Elnashai, 2001; Surana *et al.*, 2015).

Four building configurations will be used in this study: Type 1, Type 2, Type 3 and Type 4, which are illustrated in Figure 3. Only particular building types can be used to represent the low-rise, mid-rise and high-rise structures, which are dependent on the number of storeys; this is because the buildings will be initially designed for earthquake loading (using AS 1170.4) and/or wind loading (using AS 1170.2), depending on the year of construction. For example, a high-rise building may not have the (moment) capacity for the earthquake or wind demand if it only has C-shaped centralized walls (building Type 3). Therefore, HR buildings are limited to Type 4. Moreover, the single C-shaped wall building (Type 2) is limited to LR buildings designed pre-1995, before earthquake loading became a design requirement in Australia. This is because the wind loading requirement for LR buildings is typically small, and it would be unlikely that these types of buildings have the capacity when considering earthquake loading (due to the extra base shear caused from the expected torsional response). It should be noted that it is assumed that for all buildings the center of stiffness provided by the lateral load resisting walls for each principle direction is close to the center of mass; therefore, the effects of torsional displacement due to in-plane asymmetry have been neglected in this study. Moreover, LR buildings that are 1-storey high have not been included in the analyses due to the low height of the building (and corresponding cantilever walls). Thus, if 1-storey buildings were used in this analysis, a large percentage of the RC walls laterally supporting these LR buildings would result in a low aspect ratio (A_r); the RC walls that have been studied here are governed primarily by flexure and have had an A_r higher than 2. Furthermore, for this study, the C-shaped walls are assumed to be uncoupled. This assumption is only valid for moderate "high-rise" structures (less than 13-storeys), since a coupled and stiffer centralized core (boxed section) would be typical for very tall structures. Table 1 presents the different Building Types and limiting number of storeys (n).

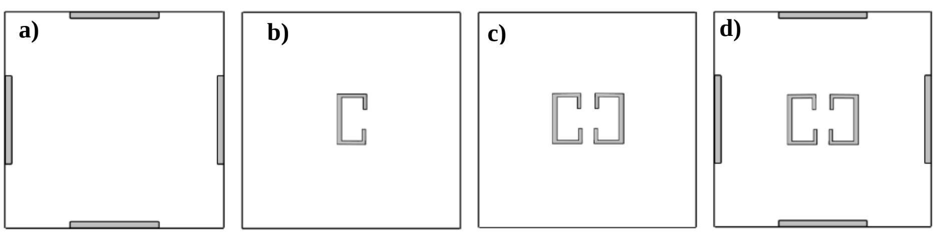

Figure 3 Building configurations (a) Type 1 (b) Type 2 (c) Type 3 and (d) Type 4

Table 1 Building Types with limiting number of storeys

Building Type	minimum n	maximum n	Rise
1	2	4	low, mid
2	2	3	low
3	2	7	low, mid
4	4	12	mid, high

The range of values used for some of the building parameters in the MATLAB assessment program are summarized in Table 2. Many of these parameters, such as material properties, are selected at random from a generated number based on a normal distribution (if a mean and standard deviation can be provided) or are randomly chosen between an appropriate minimum and maximum range. For example, the yield and ultimate stress of the reinforcing steel (f_y and f_u) are calculated from a random number using a normal distribution with a mean (μ) and standard deviation (σ) taken from the results reported in Menegon *et al*. (2015) for D500N reinforcing steel. One of the limitations to this study is the assumption that the entire RC structural wall building stock has utilised D500N reinforcing bars; due to the paucity of research and experimental testing on other types of reinforcing bars used in Australia (e.g. 230S, 410Y), D500N bars are assumed to be incorporated in the entire RC structural wall building stock. In contrast to the values for some parameters selected on the basis of a normal distribution, the axial load ratio (*ALR*), for example, is randomly chosen between a minimum of 0.01 (1%) and a maximum of 0.1 (10%), based on common values used in previous research (Henry, 2013) as well as investigations by Albidah *et al*.(2013) for low-to-moderate seismic regions and more recently Menegon *et al.* (2017) for Australia. It should be noted that other seismic assessment methodologies, such as HAZUS (FEMA, 1999) and EQRM (Robinson *et al.*, 2005), also incorporate variability of the building stock through lognormally distributed capacity functions that are calculated based on a chosen, random number. Other parameters given in Table 2 that are varied within the assessment program include the yield, hardening and ultimate strain values of the reinforcement steel (ε_{sy}, ε_{sh} and ε_{su} respectively), Young's Modulus of the reinforcing steel and concrete (E_s and E_c respectively), dead and live load of the building per floor (G and Q respectively), inter-storey height (h_s), longitudinal reinforcement ratio (ρ_{wv}), mean insitu strength of concrete (f_{cmi}) and the concrete age strength enhancement factor (κ). The length of the rectangular walls (L_w) are chosen randomly between a value of 0.17B and 0.33B, where the width of the building (B) is equal to $\sqrt{A_b}$. The dimensions of the C-shaped walls for Building Types 2, 3 and 4 in Figure 3 are based on the number of storeys; the different Building Types and range of allowable storeys (n) used in the program were given in Table 1. Moreover, the dimensions of the C-shaped walls used in the LR, MR and HR buildings correspond to that used for the numerical analyses conducted in Hoult *et al.* (2017b) (dimensions given in Table 3).

Table 2 Wall parameters and values considered for the vulnerability assessment program

Parameter	μ	σ	min	max	constant	Units
f_y	551	29.2	500	-		MPa
f_u	660.5	37.65	540	-		MPa
E_s	-	-	-	-	200,000	MPa
ε_{sy}	-	-	-	-	f_y/E_s	-
ε_{sh}	0.0197	0.0095	-	-		-

ε_{su}	0.0946	0.016	0.03	-		-
κ^a	1.5	0.4	1.2	-		-
κ^b	1.5	0.2	1.0	-		-
f_{cmi}	-	-	-	-	32κ	MPa
E_c	-	-	-	-	$5000\sqrt{f_{cmi}}$	MPa
ALR	-	-	0.01	$0.1^c/0.05^d$		-
G	-	-	4	8		kPa
Q	-	-	1	4		kPa
h_s	-	-	3.0	3.5		m
ρ_{wv}	-	-	0.19%	1.00%		-

[a] = pre-1980s buildings
[b] = post-1980s building
[c] = Rectangular walls
[d] = C-shaped Walls

Table 3 Dimensions of the C-shaped walls

Wall	t_w (mm)	L_{web} (mm)	L_{flange} (mm)	L_{return} (mm)
LR	200	3600	2000	600
MR	200	6200	2200	600
HR	250	8500	2500	600

SOIL CLASSIFICATION

Geoscience Australia conducted a study to provide a National Regolith Site Classification (NRSC) Map (McPherson & Hall, 2007) [Copyright © 2014 Risk Management Solutions, Inc. All rights reserved]. This was recognized as being an important tool for modelling earthquake events, where the map could provide information on the ‘potential influence of variation in geological materials on the ground shaking’ (McPherson & Hall, 2007). The NRSC map uses soil classifications that were defined by the shear wave velocity of the top 30 m below the surface (V_{s30}), similar to the current classification of some soils in AS 1170.4:2007 (Standards Australia, 2007). Consideration of the amplification effect by impendence (e.g. V_{s30} parameter) of the soil alone is thought be a simple and reasonable approach (Idriss, 2011; Lee & Trifunac, 2010), given the absence of other key parameters of the site conditions, such as soil thickness and fundamental site period. There is a paucity of information of both geotechnical and geophysical data in Australia (McPherson & Hall, 2013), so this method seems to be most applicable for the proposed research here. The resulting map from McPherson and Hall (2007) for Melbourne is illustrated in Figure 4 with the different colored regions corresponding to the different soil classes.

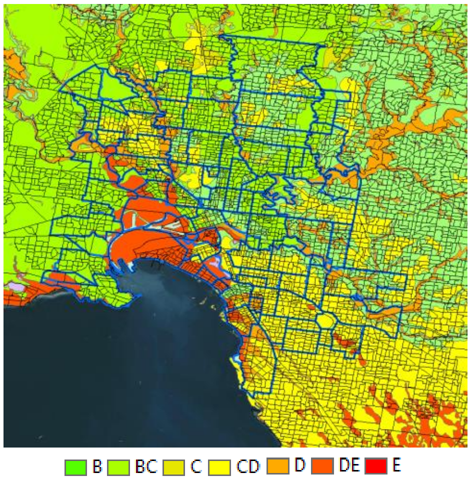

Figure 4 Soil map for Melbourne from McPherson and Hall (2007)

The NRSC map from McPherson and Hall (2007) uses seven site classes that are based on the modified NEHRP site classifications, modified by Wills *et al*. (2000) to suit the Australian conditions. These seven site classes are given in Table 4 with the associated range of V_{s30} values and "geological materials". This information can be used to estimate the site class that corresponds to AS 1170.4:2007 (Standards Australia, 2007) for each of the building locations provided by CLUE (Melbourne City Council, 2015). The site response can also be estimated using an equivalent linear analysis and shear wave velocity profiles corresponding to the modified NEHRP classes.

Table 4 Modified NEHRP (Wills *et al*., 2000) site classes applicable to Australian conditions (McPherson & Hall, 2007)

Site Class	V_{s30} (m/s)	Geological Materials
B	> 760	Fresh to moderately weather hard rock units
BC	555 - 1000	Highly weathered hard rock
C	360 - 760	Extremely weathered hard rock units
CD	270 - 555	Alluvial units
D	180 - 360	Younger alluvium
DE	90 - 270	Fine-grained alluvial, deltaic, lacustrine and estuarine deposits
E	< 180	Intertidal and back-barrier swamp deposits

EARTHQUAKE DEMAND (BUILDING DESIGN)

For this seismic assessment, the moment demand (M^*), derived from the design base shear (V_b) using the lateral loading provisions at the time of construction, will be compared to the moment capacity (M_{cap}) from the lateral load resisting elements of the building (RC walls). This initial estimate will determine if the values used for the different parameters of the walls and building, which were discussed previously, are sufficient for the buildings codes and provisions of the time and thus reflect the approximate values in the existing building stock.

Prior to the Earthquake Actions provision AS 1170.4 in 1993 (Standards Australia, 1993), the AS 2121:1979 (Standards Australia, 1979) provided some earthquake loading for structures in Australia. However, Woodside (1992) discusses how unsuccessful the code was, with the majority of buildings in Australia not requiring any specified earthquake design. Moreover, as discussed in Tsang *et al*. (2016), consideration of earthquake-resistant design in Australia has only been enforced for structures in Australia after 1995. It is for this reason that the buildings used in these analyses that have been built prior to 1995 are assumed to have only been designed for the lateral loads caused by wind.

A number of Standards could be used to determine the base shear (V_b) depending on the year built, and importantly the earthquake loading may not always govern the demand in comparison to the design wind load. Table 5 indicates what Australian Standards are used to determine the governing base shear (V_b) based on the year of construction.

Table 5 Different Standards used to determine base shear for building year

Year Built	Standard	Loading
<1983	AS 1170.2 (Standards Australia, 1975)	Wind
<1993	AS 1170.2 (Standards Australia, 1983)	Wind
<2007	AS 1170.2 (Standards Australia, 2002)	Wind
	AS 1170.4 (Standards Australia, 1993)	Earthquake
≥2007	AS 1170.2 (Standards Australia, 2011)	Wind
	AS 1170.4 (Standards Australia, 2007)	Earthquake

It should be noted that the seismic weight (W_t) of the building is calculated using Equation 1, which has been adopted from the load combination given in AS 1170.0:2002 (Standards Australia, 2002). The values for the dead load (G) and live load (Q) used in the assessment program were given in Table 2.

$$W_t = n(A_b G + 0.3 A_b Q) \tag{1}$$

The full height of the building (H_n) is determined by multiplying the number of storeys (n) by the inter-storey height (h_s). As indicated in Table 2, The h_s is randomly generated as a number between a minimum and maximum of 3.0 and 3.5 metres respectively (in increments of 0.1 metres). The area of the face of the building (A_f), used in calculating the force produced by the wind pressure, is taken as $\sqrt{A_b} H_n$. The effective height (H_e) of the building is estimated as $0.7H_n$ as recommended by Priestley *et al.* (2007) for cantilever wall structures. Thus, the moment demand (M^*) is calculated by multiplying the V_b by H_e.

BUILDING CAPACITY

The building capacity, corresponding to the ultimate moment (M_u) of the walls (reflecting current design practice in Australia), is dependent on the building type and number of RC (rectangular and/or C-shaped) walls. Moment-curvature analyses (or "section analyses") will be used to calculate the capacities of the individual walls of each building. These values will also be used in some of the plastic hinge analysis expressions to obtain the force-displacement relationship of the RC walls. Typically, a moment-curvature analysis can be undertaken using third-party computer software [e.g. RESPONSE-2000 (Bentz, 2000), XTRACT (Chadwell & Imbsen, 2004) and CUMBIA (Montejo & Kowalsky, 2007)]. However, for the purposes of this study, the moment-curvature analysis program is incorporated within MATLAB to reduce computational time associated with using a third-program. Therefore, capacities of RC rectangular and C-shaped walls and for a large range of parameters can be derived within the MATLAB assessment program, thus creating some of the variance needed to produce vulnerability functions that would represent the Australian RC structural wall building stock.

The research by Lam *et al.* (2011) will be used as a guide to produce a moment-curvature (M-Φ) program in MATLAB (Ingle & Proakis, 2016). The stress-strain (σ-ε) relationship used for the concrete and reinforcing steel is calculated using expressions given in Wong *et al.* (2013) for the Popovics (normal and high strength concrete) and Seckin (1981) (back-bone curve) models respectively.

The MATLAB M-Φ program can be used to find the ultimate moment (M_u), as well as curvature and moments at different levels of strains that correspond to different performance levels (discussed later in the paper). For the sake of brevity, the reader is referred to Lam *et al*. (2011) for a full understanding of how the M-Φ program is created. Furthermore, while the program was validated in Hoult (2017) by comparing the M-Φ output of many different walls and parameters to that obtained by third-part software, only two walls are used here to illustrate the validity of the program. The first wall is rectangular, with a wall length (L_w) of 3000 mm, thickness (t_w) of 200 mm, axial load ratio (ALR) of 5% and concrete strength (f_{cmi}) of 40 MPa. Longitudinal reinforcement ratios (ρ_{wv}) of 0.19%, 0.50%, 0.75% and 1.00% are used for the rectangular wall. The second wall is C-shaped with the dimensions given in Table 3 for the MR wall. The C-shaped wall here has a *ALR* of 5%, ρ_{wv} of 0.50% and a f_{cmi} of 40 MPa. It should be noted that the mean values of D500N bars (Table 2) were used for the properties of the reinforcing steel here. The moment-curvature results from the program written in MATLAB are given in Figure 5. Superimposed in Figure 5 are the results using RESPONSE-2000 (Bentz, 2000) and XTRACT (Chadwell & Imbsen, 2004) for the rectangular and C-shaped walls respectively. Reasonable comparisons between the estimates provided by the MATLAB *M-Φ* program and third-party software can be observed in Figure 5. Some slight inconsistencies, particularly with regards to the moment capacities of the rectangular walls in Figure 5, are likely to be due to the different material models that are incorporated in the third-party software in comparison to that used in the MATLAB *M-Φ* program.

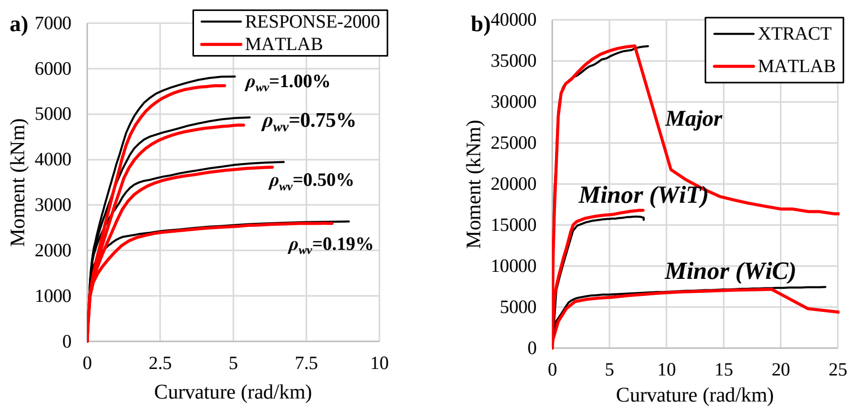

Figure 5 Moment-curvature comparisons for (a) rectangular walls and (b) C-shaped walls

Thus, the ultimate moment capacity of the building (M_u) is determined from the contribution of all walls in the building for the given direction of loading. If ΦM_u is less than M^*, where Φ is taken as 0.8 from AS 3600:2009 (Standards Australia, 2009), then the process of calculating M_u is repeated using different generated values for the parameters of the walls. This process is illustrated in the flow chart given in Figure 1. If the calculated ΦM_u of the building exceeds M^*, the program continues on to the next stage in calculating the displacement capacity of the structure.

PLASTIC HINGE ANALYSIS

A Plastic Hinge Analysis (PHA) is one of the most widely used and simplest methods for calculating the force-displacement capacities of RC members (Almeida *et al.*, 2016). The PHA acknowledges that the top displacement of a cantilever wall structure is the summation of the deformation components primarily due to flexure, shear and slipping. These deformation components can be used to calculate the yield displacement (Δ_y) and plastic displacement (Δ_p). The authors have derived several expressions for finding the Δ_y of lightly reinforced and unconfined rectangular and C-shaped walls (Hoult *et al.*, 2017a). Furthermore, several plastic hinge length (L_p) expressions have been derived from numerical analyses specifically for lightly reinforced and unconfined rectangular and C-shaped walls (Hoult *et al.*, 2017b, 2017c). These expressions are summarized below, where the reader is referred to Hoult *et al.* (2017a), Hoult *et al.* (2017b) and Hoult *et al.* (2017c) for more information on their derivation.

$$\Delta_y = K_\Delta \Phi'_y \left(\frac{k_{cr}}{3} H_n^2 + L_{yp} H_n\right)\left(1 + \frac{\Delta_s}{\Delta_f}\right) \tag{2}$$

where k_{cr} is a factor derived by Beyer (2007) and Constantin (2016) to account for the actual height of the wall estimated to be cracked (Equation 4), Δ_s / Δ_f is the shear-to-flexure deformation ratio (Equation 6), L_{yp} is the yield strain penetration length (approximately 150 mm), Φ'_y is the curvature at first yield and K_Δ is a factor introduced by Hoult *et al.* (2017a) to account for lightly reinforced walls (Equation 3).

$$K_\Delta = \theta \rho_{wv} + \beta \tag{3}$$

where the θ and β parameters are given in Table 6.

Table 6 Parameters for the K_Δ factor

		C-Shaped		
	Rectangular	Major	Minor (WiC)	Minor (WiT)
θ	45	80	50	100
β	0.22	0.00	0.30	1.00

$$k_{cr} = \alpha + 0.5(1-\alpha)\left(\frac{3H_{cr}}{H_n} - \frac{H_{cr}^2}{H_n^2}\right) \tag{4}$$

where α is the ratio of cracked to uncracked flexural wall stiffness (E_cI_{cr} / E_cI_g) and H_{cr} is the height of the cracked wall (Equation 5). It should be noted that the stiffness of the cracked section (E_cI_{cr}) can be estimated with M'_y / Φ'_y.

$$H_{cr} = \max\left(L_w, \left(1 - \frac{M_{cr}}{M'_y}\right) H_n\right) \tag{5}$$

where M_{cr} is the cracking moment and M'_y is the moment corresponding to first yield.

$$\frac{\Delta_s}{\Delta_f} = \begin{cases} 1.5\left(\frac{\varepsilon_m}{\Phi tan\theta_c}\right)\left(\frac{1}{H_e}\right), & C - shaped\ walls \\ 0, & rectangular\ walls \end{cases} \tag{6}$$

where ε_m is the mean axial strain of the RC section (which can be estimated from a moment-curvature analysis), Φ is the curvature corresponding to a performance level (discussed later in this section) and θ_c is the crack angle [with a recommended value of 30º (Priestley *et al.*, 1996) to be used for the assessment of existing structures].

$$\rho_{wv.min} = \frac{(t_w - n_t d_{bt}) f_{ct.fl}}{f_u t_w} \tag{7}$$

where $\rho_{wv.min}$ is the minimum longitudinal reinforcement required to allow secondary cracking (Hoult *et al.*, 2017c), t_w is the thickness of the wall, n_t is the number of grids of horizontal (transverse) reinforcing bars, d_{bt} is the diameter of the horizontal reinforcing bars, $f_{ct.fl}$ is the mean flexural tensile strength of the concrete and f_u is the ultimate strength of the longitudinal reinforcing bars.

$$\Phi_{pl} = \begin{cases} \frac{0.6\varepsilon_{spl} - \varepsilon_{sy}}{L_w}, & \frac{\rho_{wv}}{\rho_{wv.min}} < 1 \\ moment - curvature\ anlysis, & \frac{\rho_{wv}}{\rho_{wv.min}} \geq 1 \end{cases} \tag{8}$$

where Φ_{pl} is the curvature corresponding to a given performance level, ε_{spl} is the strain in the steel corresponding to a given performance level and L_w is the wall length.

$$L_p = \begin{cases} 150, & \frac{\rho_{wv}}{\rho_{wv.min}} < 1 \\ (\alpha L_w + \gamma H_e)(1 - \delta ALR)(\omega e^{-\tau v}), & \frac{\rho_{wv}}{\rho_{wv.min}} \geq 1 \end{cases} \tag{9}$$

where H_e is the effective height, ALR is the axial load ratio, v is the normalised shear parameter (Equation 10) and the five parameters in Equation 9 (α, γ, δ, ω and τ) are given in Table 7.

Table 7 Parameters for L_p in Equation 9

	α	γ	δ	ω	τ
Rectangular	0.1	0.075	6	1.0	0.0
C-shaped (Major)	0.1	-0.013	13	7.0	0.8
C-shaped (Minor, WiC)	0.5	-0.015	3	1.6	0.1
C-shaped (Minor, WiT)	1.0	-0.073	8	2.5	2.1

$$v = \frac{\tau}{0.17\sqrt{f_{cmi}}} \tag{10}$$

where τ is the average shear stress parameter, which can be calculated from a sectional analysis ("moment-curvature" analysis) or can be estimated by dividing the base shear (V_b) of the wall by the effective area (A_{eff}) of the section.

$$\Delta_p = L_p(\Phi_{pl} - \Phi'_y)H_e(1 + \frac{\Delta_s}{\Delta_f}) \tag{11}$$

$$\Delta_{cap} = \Delta_y + \Delta_p \tag{12}$$

The displacement capacity (Δ_{cap}) of a RC wall corresponding to different "performance levels" can thus be found. For the purposes of this research, three performance levels are used: Serviceability, Damage Control and Collapse Prevention. For reinforced concrete (RC) structures, it is common to have the maximum tensile and compressive strain values representing the engineering demand parameter (Almeida *et al.*, 2016). For example, different compressive (concrete) and tensile (steel) strain values have been recommended in Priestley *et al*. (2007) to represent when the different performance levels that are reached in RC walls. However, these strain values have been provided for well-confined reinforced concrete sections that are representative of the typical designs in high seismic regions. Therefore, the critical strain values for the different performance levels given in Priestley *et al*. (2007) for well confined concrete have been modified for use in assessing the performance of walls with the non-ductile detailing that has been commonly used in Australia. The strain values are given in Table 8, while a definition and justification for each of the values chosen to correspond to the different performance levels can be found in Hoult *et al.* (2015) and in Hoult (2017).

Table 8 Strain limits corresponding to performance levels

Structural Performance Limit State (Unconfined)	Concrete Strain	Steel Strain
Serviceability	0.001	0.005
Damage Control	0.002	.01
Collapse Prevention	0.003	.05

The Capacity Spectrum Method (CSM) will ultimately be used to assess a structure using a relationship between the calculated displacement ductility (μ) and equivalent viscous damping (ξ_{eq}) to modify the elastic acceleration and displacement demand spectra. This is to overcome one of the limitations of the CSM, as discussed in more detail later in the paper. The damping is the sum of the elastic (ξ_{el}) and hysteretic (ξ_{hyst}) damping, given in Equation 13 from Priestley *et al.* (2007) for RC cantilever wall structures.

$$\xi_{eq} = \xi_{el} + \xi_{hyst} = 0.05 + 0.444\left(\frac{\mu - 1}{\mu\pi}\right) \tag{13}$$

The ξ_{eq} is found for each of the corresponding displacements at the different performance levels. The spectral reduction factor (R_ξ) is then calculated using Equation 14, which has been adopted from the recommendations by Priestley *et al.* (2007) without considerations of forward directivity velocity pulse characteristics.

$$R_\xi = \left(\frac{0.07}{0.02 + \xi_{eq}}\right)^{0.5} \tag{14}$$

Thus, the equivalent elastic spectral displacement capacity ($\Delta_{cap.el}$) for each of the performance levels is found using Equation 15.

$$\Delta_{cap,el} = \Delta_{cap}/R_\xi \tag{15}$$

EARTHQUAKE GROUND MOTIONS

Two options will be utilized in obtaining appropriate ground motions for assessing the building stock of the Melbourne CBD. Firstly, the Pacific Earthquake Engineering Research (PEER, 2016) ground motion database was used to obtain unscaled acceleration time-histories. This is similar to the process used in Hoult *et al.* (2017e) for the site response study, although the ground motions used here are unscaled. It is important to obtain ground motions that are consistent with the geological features and faulting mechanisms that are commonly observed in Australia. A reverse fault mechanism is typically observed for earthquake events in Australia (Brown & Gibson, 2004). Moreover, the geological region of California is thought to be similar to that of the east coast of Australia (Gibson & Dimas, 2009). Using the set criteria below, the database found 13 applicable ground motions with a range of magnitude and distances.

- Magnitude (M_w) range of 5.0 to 7.5
- Reverse (and Oblique) fault types
- Rupture surface distance (R_{rup}) range of 1 km to 60 km
- V_{s30} range of 1000 m/s to 2500 m/s

The resulting record sequence numbers (RSN) of the 13 ground motions and attributes are given in Table 9 in descending order of the peak ground velocity (*PGV*) on "hard rock" (taken here as a site with V_{s30} > 1000 m/s). The *PGV* was provided in the NGA-West 2 Flatfile (Boore *et al.*, 2014) for all of the ground motions in the database. Figure 8 illustrates the wide range of spectral accelerations and displacements provided by the ground motions obtained from PEER.

Table 9 PEER (2016) ground motions used for assessing Melbourne building stock

RSN	M_w	Mechanism	R_{rup} (km)	V_{s30} (m/s)	*PGV* (mm/s)
8877	5.4	Reverse Oblique	58.5	1043.0	6.6
3718	5.3	Reverse Oblique	28.4	1222.5	6.9
643	6.0	Reverse Oblique	27.6	1222.5	15.9
1715	5.3	Reverse	17.1	1222.5	20.6
1709	5.3	Reverse	21.7	1015.9	22.8
2996	6.2	Reverse	50.4	1525.9	27.5
8167	6.5	Reverse	38.0	1100.0	84.5
1011	6.7	Reverse	20.3	1222.5	111.7
765	6.9	Reverse Oblique	9.6	1428.1	345.2
1050	6.7	Reverse	7.0	2016.1	367.7
3548	6.9	Reverse Oblique	5.0	1070.3	621.8
1051	6.7	Reverse	7.0	2016.1	755.0
77	6.6	Reverse	1.8	2016.1	755.5

Secondly, to complement the earthquake ground motions obtained from PEER (2016), artificial earthquakes were created using the program GENQKE (Lam *et al.*, 2000b), which uses a calibrated intraplate source model originally proposed by Atkinson (1993) to estimate attenuation features for the crustal properties of Melbourne (Lam *et al.*, 2006). GENQKE was also used in Tsang *et al.* (2016) to produce ground motions for the Melbourne area, where the magnitude and distance (M-R) combinations were primarily chosen based on two main "governing" faults. Tsang *et al.* (2016) found this to correspond to the Selwyn (M_{max} 7.7 and R 60km) and Muckleford faults (M_{max} 7.8 and R 120 km). However, a probabilistic seismic hazard analysis (PSHA) was conducted for the city of Melbourne using the AUS5 earthquake recurrence model (Brown & Gibson, 2004) in Hoult (2017), which found that the Muckleford fault (or "Muckleford-Leichardt" fault, as classified in the AUS5 model) did not govern the seismic hazard of the Melbourne CBD; only at very long return periods (> 10,000 years) did this fault have any contribution to the predicted seismic hazard in Melbourne. Moreover, the Beaumaris and Yarra faults were found to govern the ground motions in Melbourne for the larger return periods (2,500 to 5,000 years) in comparison to the lower return periods (< 2,500 years), where the Selwyn fault governs the hazard. Some discussions with Mr. G. Gibson (personal communication, November 1, 2016), co-author of the AUS5 earthquake recurrence model, has indicated that the Beaumaris and Yarra faults are possibly the same fault, although it has been hard to trace the fault outcrop through the

Silurian sediments that are prominent in the area. These faults, together with the Selwyn and Muckleford-Leichardt faults, have the locations and traces shown in Figure 6 (the faults discussed here traced in red, with other known faults in the area traced in yellow). Moreover, Mr. Gibson's research has found that the offset in the Port Phillip Bay coastline at Ricketts Point (the toe of the Beaumaris fault) has a significant slip rate, by Australian standards, particularly for a fault with the length of only the Beaumaris segment. This further suggests that the Beaumaris and Yarra faults are connected. The reverse fault dip of the Beaumaris fault is about 30° to 35° and will be about 10 to 12 km deep under the Melbourne CBD. Melbourne CBD is also located on the hanging wall side of the fault. Thus, the AUS5 model predicts high contributions from the Beaumaris and Yarra faults, currently modelled as two separate faults, when the model is incorporated in PSHAs. Mr. Gibson recognizes that the Selwyn fault is one of the largest in the Melbourne area, however, the fault dips away from Melbourne (to the east). This means that the Melbourne CBD is on the footwall side of the Selwyn fault, with the proximity and corresponding radiation pattern producing relatively lower ground motion in the city of Melbourne for when the Selwyn fault ruptures.

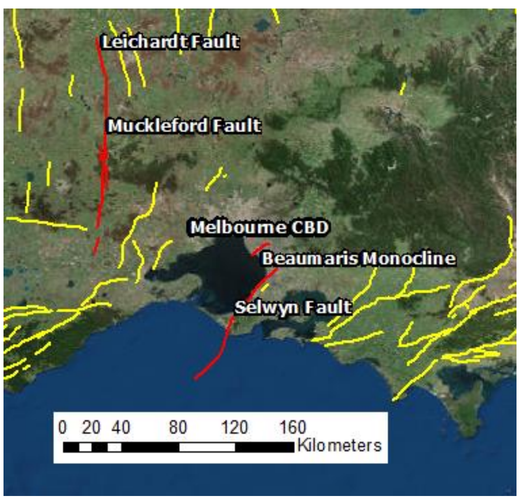

Figure 6 Greater area of Melbourne in Victoria with fault traces

Using this information, GENQKE was used to produce acceleration time-histories for a range of magnitudes (M_w of 5.0 to 7.5 in increments of 0.5) at the approximate distances of the Melbourne CBD to the Beaumaris and Yarra faults, which were 11 km and 28 km respectively. As discussed in Lam (1999), some parameters need to be chosen depending on the region of interest. A user-defined source spectrum model using the Atkinson (1993) generalised two-corner frequency format determined the stress drop parameters, originally developed for the central and eastern North America conditions. The regional dependent (Q_0) and exponent (n) factors for the Quality Factor were chosen to be 100 Hz and 0.85 respectively from the recommended values developed for the state of Victoria (Lam *et al.*, 2000a), which Melbourne is the state capital city. The crustal density (ρ_c) and crustal shear wave velocity (V_{cs}) values were chosen to be 2700 kg/m^3 and 3000 m/s respectively, based on recommendations given in Lam and Wilson (1999) and Lam *et al.* (2003). Finally, user-defined frequency and amplification factors were used for modelling the shear wave velocity gradient of the upper crust (top 3 to 4 km of crust) to coincide with using the user-defined source spectrum model from Atkinson (1993).

To illustrate the applicability of GENQKE and the parameters used above, the resulting mean of 6 artificial earthquakes produced by the program for a M-R combination of 6 and 11 km (distance from Melbourne CBD to the Beaumaris fault) is given in Figure 7. This is compared to the weighted average of the recommended ground motion prediction equations (GMPEs) that were found to be most applicable using a range of strong-motion earthquake data for the eastern region of Australia ("Non-Cratonic") in Hoult (2017) [0.3 for Allen (2012); 0.3 for Chiou and Youngs (2014); 0.2 for Atkinson and Boore (2006) B/C; 0.2 for Abrahamson *et al.* (2014)]. The results show that the acceleration time-histories produced by GENQKE give a resulting mean acceleration response that is close to the acceleration response from the weighted GMPEs. This correlation is particularly true for the period range that corresponds to most buildings (T > 0.1s). Therefore, six artificial ground motions are created for each M-R combination, where the resulting mean response spectrum (or ADRS) for each of the M-R combinations will be used for the seismic demand. Table 10 gives the mean *PGV* of the resulting artificial ground motions obtained from GENQKE using a range of magnitudes and distances, with the resulting acceleration and displacement response in Figure 8.

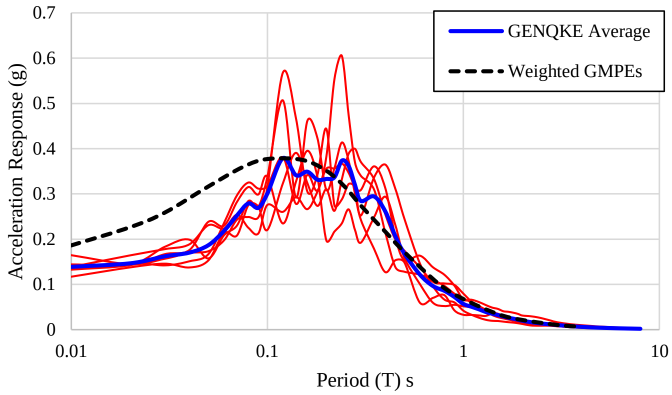

Figure 7 GENQKE M7R35 results compared to weighted GMPEs

Table 10 GENQKE ground motions used for assessing Melbourne building stock

Fault	M_w	R_{jb} (km)	*PGV* (mm/s)
Yarra	5	28	26
Yarra	5.5	28	48.3
Yarra	6	28	91.6
Beaumaris	5	11	92.2
Yarra	6.5	28	139.8
Beaumaris	5.5	11	156
Yarra	7	28	260.7
Beaumaris	6	11	294.5
Yarra	7.5	28	463.1
Beaumaris	6.5	11	471.3
Beaumaris	7	11	787.5
Beaumaris	7.5	11	1437.5

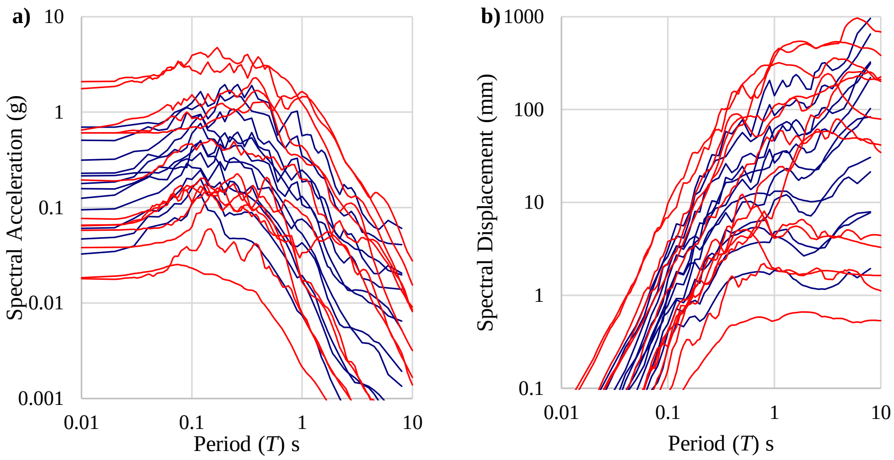

Figure 8 (a) Spectral accelerations and (b) displacements from PEER (2016) (in red) and GENQKE (Lam *et al.*, 2000b) (in blue)

SITE RESPONSE

The seismic ground motions from the bedrock can be greatly affected by the regolith material at a site (McPherson & Hall, 2013). The NRSC regolith map from McPherson and Hall (2007), discussed previously, was used such that an estimation can be made to the site conditions for each of the building locations. Furthermore, the modified NEHRP site classes (Wills *et al.*, 2000) have been used as the classification system, which have been slightly modified again for the Australian conditions (McPherson & Hall, 2007). These site classes correspond to a shear wave velocity of the upper 30 metres of crust (V_{s30}) (Table 4).

SHAKE2000 (Ordonez, 2013) is used to conduct equivalent linear analyses using the ground motions obtained in the previous section for "hard rock" conditions as inputs. The equivalent linear analyses will give estimates of the ground motion response for each of the seven different site classes according to the modified NEHRP classification. The methodology of SHAKE2000 (Ordonez, 2013) that is adopted here is given in Hoult *et al.* (2017e). It was observed in Hoult *et al.* (2017e) that the response of the ground motions atop of the soil sites were dependent on the seismic intensity, which was also observed in other studies (Amirsardari *et al.*, 2016; Dhakal *et al.*, 2013; Walling *et al.*, 2008). This dependency is not currently reflected in design codes, such as the AS 1170.4:2007 (Standards Australia, 2007), and therefore using site amplification from the Standards (or spectral shape factors) would likely lead to an inaccurate estimate of the site response. Using equivalent linear analyses for all of these ground motions (given in Table 9 and Table 10), while an onerous process, will provide a much more accurate estimate of the expected site response.

To provide an estimate of site response using SHAKE2000 (Ordonez, 2013), a shear wave velocity (V_s) profile is required. The average shear wave velocity of the upper 30 meters of crust (V_{s30}) must correspond to one of the seven different soil classes (according to the modified NEHRP classification) that are prevalent around Melbourne, as shown in Figure 4. The V_{s30} can be calculated using Equation 16:

$$V_{s30} = 30/\sum_{i=1}^{n}\left(\frac{h_i}{S_i}\right) \tag{16}$$

where h_i is the thickness of sediment layer i, S_i is the shear-wave velocity layer i and n is the total number of sediment layers (McPherson & Hall, 2013).

Although the shear wave velocity profile will vary between sites, due to the limitations of data resources it is assumed that the following shear wave velocity profiles are representative of typical profiles for the different soil classes in Melbourne. Four V_s profiles were obtained from Roberts *et al*. (2004) based on a study that investigated different soil profiles around the Melbourne area. Each of these four V_s profiles correspond to one of the different soil classes (*B*, *BC*, *C* and *CD*) as defined in McPherson and Hall (2007). Profiles obtained from the Melbourne area corresponding to soil classes *D*, *DE* and *E* were scarce. However, the soil classes of *D* and *DE* located in Melbourne are primarily associated with alluvial and shoreline sand deposits, which is similar to those found in Sydney (McPherson & Hall, 2007). Therefore, two V_s profiles were obtained from Kayen *et al*. (2015), which are taken from site studies conducted in the city of Sydney. Moreover, a shear wave velocity profile corresponded to soil class *E* from Newcastle (Kayen *et al.*, 2015) is subsequently used here. The calculated and reported V_{S30} of the seven soil profiles used for this assessment are given in Table 11.

Table 11 V_s profiles and corresponding site classes used for this study

Profile	Site Class	Reported V_{s30} (m/s)	Calculated V_{s30} (m/s)
Burnley, Melbourne	*B*	-	870.7
Royal Park, Melbourne	*BC*	-	901.2
Trinity College, Melbourne	*C*	-	649.7
Monash, Melbourne	*CD*	-	487.5
Rosebery, Sydney	*D*	314	320.9
Botany, Sydney	*DE*	250	251.1
Wickham Park, Newcastle	*E*	177	175.3

Equivalent linear analyses were undertaken using the 25 ground motions given in previous section for the seven different V_s profiles given above. The same procedure, including the models and input values, from the analyses using SHAKE2000 (Ordonez, 2013) in Hoult *et al.* (2017e) were used here. It should be noted that a rock material was assumed for soil class *B*, while a clay material was used for site classes *BC*, *C* and *D*, instead of sand, due to results from Hoult *et al.* (2017e) indicating that the response from clay is typically larger than sand sites; a conservative response was warranted for this study. Furthermore, a sand material was used for the entire profile of site classes *D*, *DE* and *E*, as these soil classes are commonly attributed to deep alluvial sites for Melbourne (McPherson & Hall, 2007). More information on the models and values for different parameters used in SHAKE2000 (Ordonez, 2013) can be found in Hoult *et al.* (2017e).

The acceleration response at the surface of the soil deposits were calculated for all 25 ground motions. Thus, the acceleration and displacement response spectra (ADRS) can be used in assessing a building for the various soil conditions that surround the Melbourne CBD. For the sake of brevity, only one of the site response results (acceleration and displacement response), but for all site classes, is given in Figure 9 as an example of output, where the M-R combination of 6 and 28 km was used (artificial ground motions from the Yarra fault).

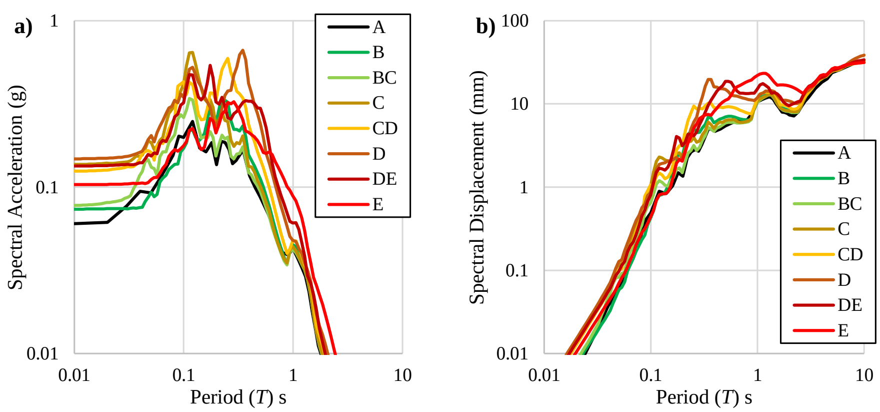

Figure 9 Site response results for Yarra fault (M6R28) (a) acceleration and (b) displacement response

CAPACITY SPECTRUM METHOD

The Capacity Spectrum method (CSM) will be used to assess the buildings. The CSM was first developed by Freeman *et al*. (1975), Freeman (1978) and Freeman (1998) and has gained a considerable amount of popularity internationally for assessing a building for seismic loading (Wilson & Lam, 2003). This is primarily due to its simplicity in comparison to the more rigorous, time consuming and (typically) computationally expensive methods, such as conducting nonlinear dynamic time-history analyses. The method commonly involves comparing the capacity curve of a structure to the seismic demand in the format of an acceleration-displacement response spectrum (ADRS). This method is illustrated in Figure 10, which shows the plotted capacity curve for a generic structure compared to a demand curve in the format of ADRS. The "performance point" (or "demand point" in Figure 10) is the location on the graph at which the two curves intersect (with the same effective damping), which provides an estimation of both the inelastic acceleration and displacement demand of a structure for a given earthquake. Some limitations of the Capacity Spectrum method include the idealization of multi-degree-of-freedom (MDOF) to single-degree-of-freedom (SDOF), which (as previously discussed) is potentially not suitable for some tall or irregular structures where higher mode effects can be substantial. There have been some proposals for modifications of the method to include higher mode effects (Bracci *et al.*, 1997; Gupta & Kunnath, 2000; Humar *et al.*, 2011; Paret *et al.*, 1996). Mehdipanah *et al*. (2016) found that a 'generalised lateral force method' was robust in comparison to the results using response spectrum analysis for a large range of asymmetric RC buildings less than 30 metres in height. Therefore, it is suggested, as has been acknowledged previously, for the purposes of the proposed study the buildings be restricted to 12-storeys in height (e.g. for "High-Rise" buildings) if the structures are to be idealized using a PHA. Another limitation of the CS method is the inherent belief that the seismic deformation of an inelastic SDOF system can be reasonably estimated by using an equivalent linear SDOF system. This estimation then requires an iterative process of varying the equivalent viscous damping to ultimately avoid the dynamic analysis of the inelastic SDOF (or MDOF) system (Chopra & Goel, 1999). However, an estimate can be provided using the method and expressions given previously in Plastic Hinge Analysis section.

For regular buildings of limited height, the CS method can be 'the most economical solution at the moment' (Causevic & Mitrovic, 2011) and is used in a range of seismic risk assessment programs (FEMA, 2010; Robinson *et al.*, 2005). It has also been implemented in a number of different international seismic design codes (ATC, 1996; Eurocode 8, 2004; FEMA, 2005).

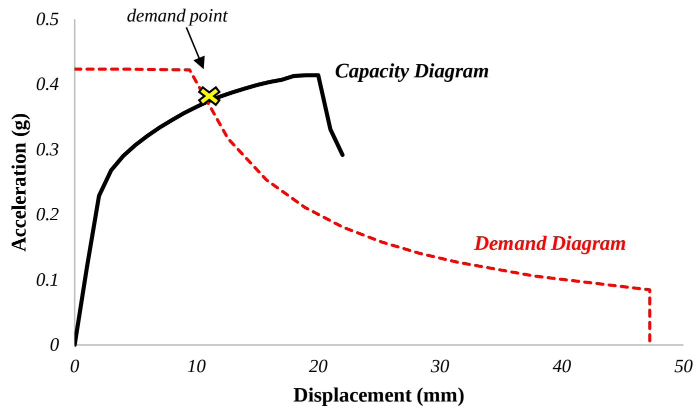

Figure 10 The capacity spectrum method

VULNERABILITY FUNCTIONS

The cumulative probability of a building reaching or exceeding a specified performance level (Table 8) for a given intensity measure (*IM*) or engineering demand parameter, such as peak ground velocity (*PGV*), is a function of the structures vulnerability. The vulnerability function, which is also loosely referred to as a fragility curve (or function), commonly conforms closely to a lognormal function. This implies that the intensity values of the ground motions that cause a particular building to reach or exceed a given performance level (e.g. Collapse Prevention) are lognormally distributed, which is a reasonable assumption that has been confirmed in a number of observed cases according to Baker (2015). Previous research has shown that vulnerability functions can effectively quantify the seismic vulnerability of structures (Aslani & Miranda, 2005; Brown & Lowes, 2007; Gulec *et al.*, 2010; Pagni & Lowes, 2006; Sengupta & Li, 2016).

The lognormal cumulative distribution function is calculated using Equation 17 (Baker, 2015):

$$P(di|IM = x) = \sigma\left(\frac{\ln\left(\frac{x}{\theta}\right)}{\beta}\right) \tag{17}$$

where $P(di|IM = \mathrm{x})$ is the probability that a ground motion, or intensity, with $IM = x$ will cause the building to reach a particular damage state (di), σ is the standard normal cumulative distribution function, θ is the median or the IM level with a 50% probability of reaching the damage state, and β is the standard deviation of $\ln(IM)$.

A reasonable approximation is typically made for the median (θ) and standard deviation (β) in order to calculate the normal distribution value for a given *IM* value. These values are then varied to provide the best fit to the data using the calculations below. As explained in Baker (2015), deriving fragility curves from the multiple stripe analysis (MSA) approach is ideal when a selected number of ground motions have been chosen to represent a specific site and *IM* level. This is equivalent to what is proposed with the study for this research; to derive fragility curves of the RC structural wall building stock of Australia using a site-specific study (e.g. Melbourne). The MSA approach is ideal for the dataset that will be used for the proposed study, as the 'analysis need not be performed up to *IM* amplitudes where all ground motions cause collapse' (Baker, 2015). The method of calculating fragility curves using the MSA approach is given in Baker (2015), where the logarithm likelihood function has been maximized and expressed in the form of Equation 18. It should be noted that a binominal distribution is used to calculate the probability of observing z_j collapses out of n_j ground motions ($IM = x_j$). Furthermore, it should also be noted that in the case of many buildings being assessed as opposed to just one structure, as is with the proposed study here, the same calculations conducted by Shinozuka *et al*. (2001) for preparing the data used for the cumulative binomial distribution will be adopted for the MSA approach described above.

$$\{\hat{\theta}, \hat{\beta}\} = \arg\max(\theta, \beta) \sum_{j=1}^{m} \left\{ \ln \binom{n_j}{p_j} + z_j \ln \sigma \left(\frac{\ln\left(\frac{x}{\theta}\right)}{\beta} \right) + (n_j - z_j) \ln \left(1 - \sigma \left(\frac{\ln\left(\frac{x}{\theta}\right)}{\beta} \right) \right) \right\} \tag{18}$$

where p_j is the 'probability that a ground motion with $IM = x_j$ will cause collapse of the structure' and '*m* is the number of *IM* levels and Π denotes a product over all levels' (Baker, 2015).

Commented [EL1]: The definition seems inappropriate for this particular equation
Π is not in the eq in this form

RESULTS AND DISCUSSION

The vulnerability function results from the assessment program written in MATLAB for LR, MR and HR RC shear wall buildings are illustrated in Figure 11, Figure 12 and Figure 13 respectively. These figures show the expected Damage Index (probability of reaching or exceeding a given performance level) as a function of the intensity of the earthquake event, where *PGV* and Modified Mercalli Intensity (MMI) have been used as the *IM*. The *PGV* was converted to MMI using Equation 19 from Newmark and Rosenblueth (1971). Table 12 provides the resulting median (θ) and standard deviation (β) parameters for the vulnerability functions derived from the MATLAB assessment program.

$$2^I = \left(\frac{7}{5}\right) PGV \qquad (19)$$

In 2014, Geoscience Australia (GA) released a report of the southeast Asian regional workshop on structural vulnerability models for the Global Risk Assessment (“GAR15”) project (Maqsood *et al.*, 2014). This report included vulnerability curves for several different classifications of structures subjected to earthquakes. The vulnerability curves for LR, MR and HR RC shear wall low resistance buildings have been superimposed in Figure 11, Figure 12 and Figure 13 respectively. It should be noted that “low resistance” buildings, as classified in Maqsood *et al*. (2014), are ‘compatible with low local seismicity with a bedrock *PGA* <=0.1g with increasing variability of performance in an urban population of buildings’, which is within the peak ground acceleration (*PGA*) values currently used to design buildings of “normal importance” (ABCB, 2016) in all capital cities throughout Australia (Standards Australia, 2007). If one reasonably assumes that the curves from Maqsood *et al.* (2014) represent a near “collapse prevention” performance level, then the vulnerability functions derived from the research conducted here indicates a more vulnerable RC shear wall building stock for lower intensity earthquake events (e.g. *PGV* < 150 – 200 mm/s) in comparison to the curves from Maqsood *et al.* (2014). This observation is particularly true for the LR and MR buildings.

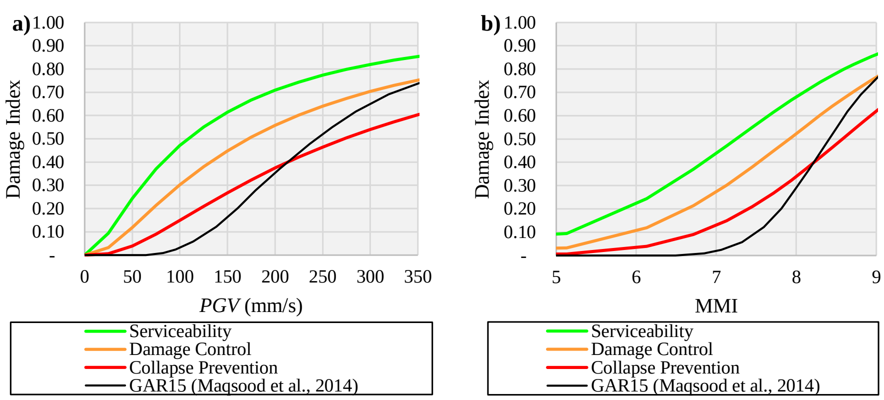

Figure 11 Vulnerability functions for LR RC structural wall buildings for an intensity measure of (a) *PGV* and (b) MMI

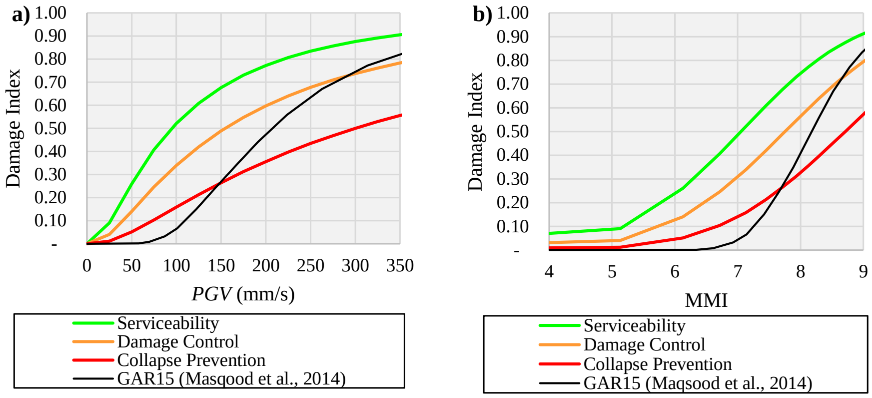

Figure 12 Vulnerability functions for MR RC structural wall buildings for an intensity measure of (a) *PGV* and (b) MMI

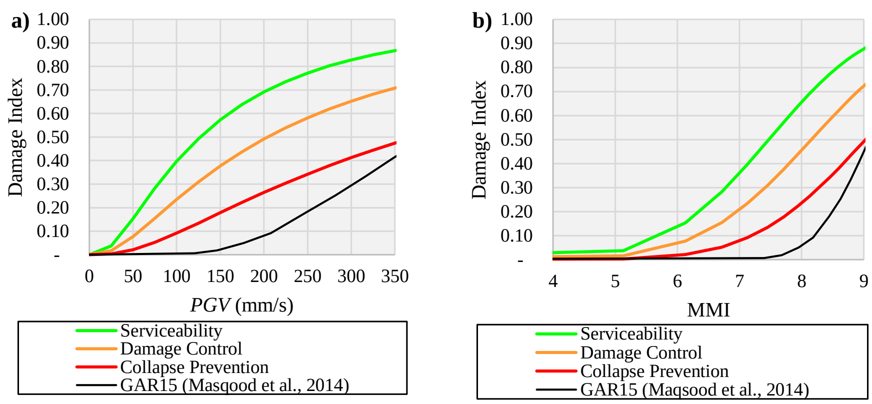

Figure 13 Vulnerability functions for HR RC structural wall buildings for an intensity measure of (a) *PGV* and (b) MMI

Table 12 Median (θ) and Standard Deviation (β) values for fragility curves (where $IM = PGV$)

	Serviceability		Damage Control		Collapse Prevention	
	θ	β	θ	β	θ	β
LR	108.4	1.11	171.8	1.04	272.4	0.96
MR	94.9	1.00	154.4	1.05	299.8	1.10
HR	126.8	0.91	204.1	0.98	373.3	0.99

Although the results from this study are specific to the RC shear wall building stock of Melbourne, the observed damage distributions from the 1989 Newcastle earthquake can be used for some comparisons to the results here. The Newcastle main earthquake event was estimated to be of local magnitude (M_L) 5.6 (McCue *et al.*, 1990). No strong ground motion recording of the main event exists as there were no instruments installed close to the epicenter of the Newcastle earthquake at the time of rupture (Chandler *et al.*, 1991; Melchers, 1990). However, the synthetic ground motions predicted by Sinadinovski *et al.* (2000) to replicate the Newcastle main event estimated *PGV* values within the range of 40 mm/s to 50 mm/s. If a value of *PGV* of 50 mm/s is assumed to correspond to the Newcastle main event, the result using Figure 11(a) predict that approximately 24%, 12% and 4% of LR RC shear wall buildings would reach (or exceed) the performance levels of Serviceability, Damage Control and Collapse Prevention (respectively) in such an event. In the research conducted by Chandler *et al.* (1991), it was documented that approximately 19%, 10% and 3% of (commercial) 'RC Frame' buildings reached "damage levels" of D4, D3 and D2, the large majority of which were LR structures. Given that the definitions of the different damage levels from Chandler *et al.* (1991) (given in Table 13) are similar to the definitions of the performance levels used in this research, it is interesting to note the close correlations of damage index observed from the Newcastle earthquake to the estimates from the functions derived in this research. It is also worth noting that for a *PGV* of 50 mm/s, the function from Maqsood *et al.* (2014) predicts a damage index of zero (Figure 11a).

Table 13 Definition of damage levels (Chandler *et al*., 1991)

	Damage State	Definition
D0	Undamaged	No visible damage
D1	Slight Damage	Infill panels damages
D2	Moderate Damage	Cracks < 10 mm in structure
D3	Heavy Damage	Heavy damage to structural members, loss of concrete
D4	Partial Destruction	Complete collapse of individual structural member or major deflection to frame
D5	Collapse	Failure of structural members to allow fall of roof or slab

CONCLUSIONS

The RC structural wall building stock in the Melbourne CBD was assessed using the Capacity Spectrum method. Importantly, plastic hinge analyses were conducted to find the capacity (load versus displacement behavior) of the buildings in comparison to adopting generic building parameters, such as the assessments that are typically conducted in HAZUS (FEMA, 2010) or EQRM (Robinson *et al.*, 2005). Building stock information from the CLUE dataset was utilized to idealize the structures into four different types which utilized rectangular and/or C-shaped walls as their lateral load resisting elements. Real and artificial acceleration time-histories were used to represent a wide range of applicable ground motions for the region. Equivalent linear analyses were conducted to find the site response of those ground motions using seven shear wave velocity profiles corresponding to the modified NEHRP soil classes. Thus, the vulnerability functions for the LR, MR and HR RC shear wall buildings were derived. It was shown that the derived functions estimate a more vulnerable building stock for low-to-moderate seismic events (e.g. $PGV < 200$ mm/s) in comparison to the vulnerability estimates by others [e.g. Maqsood *et al.* (2014)].

It should also be noted that the same assessment procedure used here was also used in Hoult *et al.* (2017d) to indicate the expected Collapse Prevention (CP) damage distribution from 500-year and 2500-year return period (RP) earthquake scenarios. The results in Hoult *et al.* (2017d) showed that a small percentage (2.4%) of the analyzed building stock was estimated in reaching (or exceeding) the CP performance level for the 500-year RP. However, an estimated 38.5% of the building stock reached the CP performance level for the 2500-year RP event. These results emphasize the vulnerability of these buildings to a very rare earthquake event and that there would currently be a substantial loss of life and considerable economic loss associated with such an event. The world's best practice for places of low-to-moderate seismicity is to construct performance objectives that specifically aim to ensure collapse prevention under very rare events in seismic design. The research results here indicate that the Australian building code board should also follow this. Importantly, the requirements for detailing of reinforced concrete walls specified in AS 3600:2009 (Standards Australia, 2009) have been shown to be inadequate and changes are needed to ensure that sufficient displacement capacity is provided. For these reasons it is strongly recommended that the Building Code of Australia (ABCB, 2016) be amended so it requires a performance objective of collapse prevention under a 2500-year return period earthquake.

ACKNOWLEDGEMENTS

The support of the Commonwealth of Australia through the Cooperative Research Centre program is acknowledged.

REFERENCES

ABCB. (2016). The National Construction Code (NCC) 2016 Buildings Code of Australia - Volume One: Australian Building Code Board (ABCB).

Abrahamson, N., Silva, W., & Kamai, R. (2014). Summary of the ASK14 Ground-Motion Relation for Active Crustal Regions. *Earthquake Spectra*. doi:10.1193/070913EQS198M

Albidah, A., Altheeb, A., Lam, N., & Wilson, J. (2013). *A Reconnaissance Survey on Shear Wall Characteristics in Regions of Low-to-Moderate Seismicity*. Paper presented at the Paper presented at the Australian Earthquake Engineering Society 2013 Conference, Hobart, VIC.

Allen, T. (2012). Stochastic ground motion prediction equations for southeastern Australian earthquakes using updated source and attenuation parameters. *Geoscience Australia Record, 69*.

Almeida, J. P., Tarquini, D., & Beyer, K. (2016). Modelling Approaches for Inelastic Behaviour of RC Walls: Multi-level Assessment and Dependability of Results. *Archives of Computational Methods in Engineering, 23*(1), 69-100.

Amirsardari, A., Goldsworthy, H. M., & Lumantarna, E. (2016). Seismic Site Response Analysis Leading to Revised Design Response Spectra for Australia. *Journal of Earthquake Engineering*, 1-30. doi:10.1080/13632469.2016.1210058

Aslani, H., & Miranda, E. (2005). Fragility assessment of slab-column connections in existing non-ductile reinforced concrete buildings. *Journal of Earthquake Engineering, 9*(06), 777-804.

ATC. (1996). Seismic evaluation and retrofit of concrete buildings. *Applied Technology Council, report ATC-40. Redwood City*.

Atkinson, G. M. (1993). Earthquake source spectra in eastern North America. *Bulletin of the Seismological Society of America, 83*(6), 1778-1798.

Atkinson, G. M., & Boore, D. M. (2006). Earthquake Ground-Motion Prediction Equations for Eastern North America. *Bulletin of the Seismological Society of America, 96*(6), 2181-2205. doi:10.1785/0120050245

Baker, J. W. (2015). Efficient Analytical Fragility Function Fitting Using Dynamic Structural Analysis. *Earthquake Spectra, 31*(1), 579-599.

Beca. (2011). *Investigation into the collapse of the Pyne Gould Corporation Building on 22nd February 2011, Report. 46 pp.* Retrieved from

Bentz, E. C. (2000). RESPONSE-2000: Sectional Analysis of Reinforced Concrete Members (Version 1.0.5). University of Toronto. Retrieved from http://www.ecf.utoronto.ca/~bentz/r2k.htm

Beyer, K. (2007). *Seismic design of torsionally eccentric buildings with U-shaped RC Walls.* (PhD), ROSE School. (ROSE-2008/0X)

Boore, D. M., Stewart, J. P., Seyhan, E., & Atkinson, G. M. (2014). NGA-West2 equations for predicting PGA, PGV, and 5% damped PSA for shallow crustal earthquakes. *Earthquake Spectra, 30*(3), 1057-1085.

Bracci, J. M., Kunnath, S. K., & Reinhorn, A. M. (1997). Seismic performance and retrofit evaluation of reinforced concrete structures. *Journal of Structural Engineering, 123*(1), 3-10.

Brown, A., & Gibson, G. (2004). A multi-tiered earthquake hazard model for Australia. *Tectonophysics, 390*(1–4), 25-43.

Brown, P. C., & Lowes, L. N. (2007). Fragility functions for modern reinforced-concrete beam-column joints. *Earthquake Spectra, 23*(2), 263-289.

Causevic, M., & Mitrovic, S. (2011). Comparison between non-linear dynamic and static seismic analysis of structures according to European and US provisions. *Bulletin of Earthquake Engineering, 9*(2), 467-489.

CERC. (2012). Canterbury Earthquakes Royal Commission. Final report: Volume 2: The performance of Christchurch CBD Buildings. Wellington, NZ.

Chadwell, C. B., & Imbsen, R. A. (2004). XTRACT: A Tool for Axial Force - Ultimate Curvature Interactions *Structures 2004* (pp. 1-9).

Chandler, A., Pappin, J., & Coburn, A. (1991). Vulnerability and seismic risk assessment of buildings following the 1989 Newcastle, Australia earthquake. *Bulletin of the New Zealand National Society for Earthquake Engineering, 24*(2), 116-138.

Chiou, B., & Youngs, R. (2014). Update of the Chiou and Youngs NGA Model for the Average Horizontal Component of Peak Ground Motion and Response Spectra. *Earthquake Spectra*. doi:10.1193/072813EQS219M

Chopra, A. K., & Goel, R. K. (1999). Capacity-demand-diagram methods based on inelastic design spectrum. *Earthquake Spectra, 15*(4), 637-656.

Constantin, R. (2016). *Seismic behaviour and analysis of U-shaped RC walls.* École polytechnique fédérale de Lausanne, Lausanne, Switzerland.

Dhakal, R. P., Lin, S. L., Loye, A. K., & Evans, S. J. (2013). Seismic design spectra for different soil classes. *Bulletin of the NZ Society of Earthquake Engineering, 46*(2), 79-87.

Edwards, M., Robinson, D., McAneney, K., & Schneider, J. (2004). *Vulnerability of residential structures in Australia.* Paper presented at the 13th World Conference on Earthquake Engineering, Vancouver. Paper.

Eurocode 8. (2004). Design of structures for earthquake resistance. Part 1: general rules, seismic actions and rules for buildings. In E. S. E. 1998-1:2004 (Ed.). Brussels, Belgium, 2004: Comit´e Europ´een de Normalisation.

FEMA. (1999). HAZUS99 User's Manual. Federal Emergency Management Agency. Washington, DC. .

FEMA. (2003). HAZUS-MH MR4 user manual, multi-hazard loss estimation methodology earthquake model: FEMA 366, Washington, DC.

FEMA. (2005). *Improvement of nonlinear static seismic analysis procedures*: Washington, D.C. : Dept. of Homeland Security, Federal Emergency Management Agency, [2005].

FEMA. (2010). HAZUS MH MR5 Technical Manual. Washington, D.C.

Freeman, S., Nicoletti, J., & Tyrell, J. (1975). *Evaluations of existing buildings for seismic risk–A case study of Puget Sound Naval Shipyard, Bremerton, Washington.* Paper presented at the Proceedings of the 1st US National Conference on Earthquake Engineering.

Freeman, S. A. (1978). Prediction of response of concrete buildings to severe earthquake motion. *Special Publication, 55*, 589-606.

Freeman, S. A. (1998). *The capacity spectrum method as a tool for seismic design.* Paper presented at the Proceedings of the 11th European conference on earthquake engineering.

Gibson, G., & Dimas, V. (2009). *Earthquake Hazard at Newcastle*. Paper presented at the Australian Earthquake Engineering Society 2009 Conference, Newcastle, New South Wales.

Gulec, C. K., Whittaker, A. S., & Hooper, J. D. (2010). Fragility functions for low aspect ratio reinforced concrete walls. *Engineering Structures, 32*(9), 2894-2901.

Gupta, B., & Kunnath, S. K. (2000). Adaptive spectra-based pushover procedure for seismic evaluation of structures. *Earthquake Spectra, 16*(2), 367-392.

Hancock, J., & Bommer, J. J. (2007). Using spectral matched records to explore the influence of strong-motion duration on inelastic structural response. *Soil Dynamics and Earthquake Engineering, 27*(4), 291-299. doi:http://dx.doi.org/10.1016/j.soildyn.2006.09.004

Henry, R. S. (2013). Assessment of the Minimum Vertical Reinforcement Limits for RC Walls. *Bulletin of the New Zealand Society for Earthquake Engineering, 46*(2), 88.

Hoult, R. (2017). *Seismic assessment of reinforced concrete walls in Australia.* (PhD), University of Melbourne. Retrieved from http://hdl.handle.net/11343/192443

Hoult, R., Goldsworthy, H., & Lumantarna, E. (2017a). Displacement Capacity of Lightly Reinforced and Unconfined Concrete Structural Walls. *Manuscript submitted for publication.*

Hoult, R., Goldsworthy, H., & Lumantarna, E. (2017b). Plastic Hinge Length for Lightly Reinforced C-shaped Concrete Walls. *Manuscript submitted for publication.*

Hoult, R., Goldsworthy, H., & Lumantarna, E. (2017c). Plastic Hinge Length for Lightly Reinforced Rectangular Concrete Walls. *Journal of Earthquake Engineering*. doi:10.1080/13632469.2017.1286619

Hoult, R. D., Goldsworthy, H. M., & Lumantarna, E. (2015, 1-3 September). *Improvements and difficulties associated with the seismic assessment of infrastructure in Australia.* Paper presented at the Australasian Fire and Emergency Service Authorities Council (AFAC) 2015 conference, Adelaide, South Australia.

Hoult, R. D., Goldsworthy, H. M., & Lumantarna, E. (2017d). *Seismic Assessment of the RC building stock of Melbourne from rare and very rare earthquake events*. Paper presented at the Australian Earthquake Engineering Society 2017 Conference, Canberra, ACT.

Hoult, R. D., Lumantarna, E., & Goldsworthy, H. M. (2017e). Soil amplification in low-to-moderate seismic regions. *Bulletin of Earthquake Engineering, 15*(5), 1945-1963. doi:10.1007/s10518-016-0067-5

Humar, J., Fazileh, F., Ghorbanie-Asl, M., & Pina, F. E. (2011). Displacement-based seismic design of regular reinforced concrete shear wall buildings. *Canadian Journal of Civil Engineering, 38*(6), 616-626.

Idriss, I. (2011). *Use of VS30 to represent local site condition*. Paper presented at the 4th IASPEI/IAEE International Symposium: Effects of Surface Geology on Strong Ground-motion.

Ingle, V. K., & Proakis, J. G. (2016). *Digital Signal Processing Using MATLAB: A Problem Solving Companion*: Cengage Learning.

Kayen, R. E., Carkin, B. A., Allen, T., Collins, C., McPherson, A., & Minasian, D. L. (2015). *Shear-wave velocity and site-amplification factors for 50 Australian sites determined by the spectral analysis of surface waves method* (2331-1258). Retrieved from

Lam, N., Sinadinovski, C., Koo, R., Wilson, J. L., & Doherty, K. (2003). Peak ground velocity modelling for Australian intraplate earthquakes. *Journal of Seismology and Earthquake Engineering, 5*(2), 11-22.

Lam, N., Venkatesan, S., Wilson, J., Asten, M., Roberts, J., Chandler, A., & Tsang, H. H. (2006). Generic Approach for Modelling Earthquake Hazard. *Advances in Structural Engineering, 9*(1), 67-82. doi:10.1260/136943306776232963

Lam, N., Wilson, J., Chandler, A., & Hutchinson, G. (2000a). Response spectral relationships for rock sites derived from the component attenuation model. *Earthquake Engineering & Structural Dynamics, 29*(10), 1457-1489.

Lam, N., Wilson, J., & Hutchinson, G. (2000b). Generation of synthetic earthquake accelerograms using seismological modelling: A review. *Journal of Earthquake Engineering, 4*(3), 321-354. doi:10.1080/13632460009350374

Lam, N., Wilson, J., & Lumantarna, E. (2011). Force-deformation behaviour modelling of cracked reinforced concrete by EXCEL spreadsheets. *Computers and Concrete, 8*(1), 43-57.

Lam, N. T. K. (1999). Program'GENQKE'User's Guide. *Department of Civil and Environmental Engineering, The University of Melbourne, Australia*.

Lee, V. W., & Trifunac, M. D. (2010). Should average shear-wave velocity in the top 30m of soil be used to describe seismic amplification? *Soil Dynamics and Earthquake Engineering, 30*(11), 1250-1258.

Lestuzzi, P., & Bachmann, H. (2007). Displacement ductility and energy assessment from shaking table tests on RC structural walls. *Engineering Structures, 29*(8), 1708-1721. doi:http://dx.doi.org/10.1016/j.engstruct.2006.09.009

Maqsood, T., Wehner, M., Ryu, H., Edwards, M., Dale, K., & Miller, V. (2014). GAR15 Regional Vulnerability Functions *Record 2014/38*: Geoscience Australia: Canberra.

McCue, K., Wesson, V., & Gibson, G. (1990). Seismological Aspects of the Newcastle NSW Earthquake of 28 December 1989. *Conference on the Newcastle Earthquake: Conference Proceedings*, 9.

McPherson, A., & Hall, L. (2013). Site Classification for Earthquake Hazard and Risk Assessment in Australia. *Bulletin of the Seismological Society of America, 103*(2A), 1085-1102. doi:10.1785/0120120142

McPherson, A. A., & Hall, L. S. (2007). Development of the Australian national regolith site classification map (pp. 37): Geoscience Australia Record 2007/07.

Mehdipanah, A., Lam, N., & Lumantarna, E. (2016). *Behaviour of Buildings featuring Transfer Beams in the Regions of Low to Moderate Seismicity*. Paper presented at the Australasian Structural Engineering Conference 2016, Brisbane, Australia.

Melbourne City Council. (2015). *Census of land use and employment*. Retrieved from: https://data.melbourne.vic.gov.au/clue

Melchers, R. (1990). Newcastle earthquake study. *The Institute of Engineers Australia*.

Menegon, S. J., Tsang, H. H., & Wilson, J. L. (2015). *Overstrength and ductility of limited ductile RC walls: from the design engineers perspective*. Paper presented at the Proceedings of the Tenth Pacific Conference on Earthquake Engineering, Sydney, Australia.

Menegon, S. J., Wilson, J. L., Lam, N. T. K., & Gad, E. F. (2017). RC walls in Australia: reconnaissance survey of industry and literature review of experimental testing. *Australian Journal of Structural Engineering, 18*(1), 24-40. doi:10.1080/13287982.2017.1315207

Montejo, L. A., & Kowalsky, M. J. (2007). CUMBIA—Set of codes for the analysis of reinforced concrete members. *CFL Technical Rep. No. IS-07, 1*.

Morris, G. J., Bull, D. K., & Bradley, B. A. (2015). In Situ Conditions Affecting the Ductility Capacity of Lightly Reinforced Concrete Wall Structures in the Canterbury Earthquake Sequence. *Bulletin of the NZ Society of Earthquake Engineering, 48*(3), 191-204.

Mwafy, A. M., & Elnashai, A. S. (2001). Static pushover versus dynamic collapse analysis of RC buildings. *Engineering Structures, 23*(5), 407-424. doi:http://dx.doi.org/10.1016/S0141-0296(00)00068-7

Newmark, N. M., & Rosenblueth, E. (1971). Fundamentals of earthquake engineering. *Civil engineering and engineering mechanics series, 12*.

Ordonez, G. A. (2013). SHAKE2000 (Version 9.99.2 - July 2013). Retrieved from http://www.geomotions.com

Pagni, C. A., & Lowes, L. N. (2006). Fragility functions for older reinforced concrete beam-column joints. *Earthquake Spectra, 22*(1), 215-238.

Paret, T. F., Sasaki, K. K., Eilbeck, D. H., & Freeman, S. A. (1996). *Approximate inelastic procedures to identify failure mechanisms from higher mode effects.* Paper presented at the Proceedings of the eleventh world conference on earthquake engineering.

PEER. (2016). Pacific Earthquake Engineering Research (PEER) Center Ground Motion Database, from http://ngawest2.berkeley.edu.

Priestley, M. J. N., Calvi, G. M., & Kowalsky, M. J. (2007). *Displacement-based seismic design of structures / M. J. N. Priestley, Gian Michele Calvi, Mervyn J. Kowalsky*: Pavia : IUSS Press : Fondazione Eucentre, 2007.

Priestley, M. J. N., Seible, F., & Calvi, G. M. (1996). *Seismic design and retrofit of bridges*: New York : Wiley, c1996.

Roberts, J., Asten, M., Tsang, H. H., Venkatesan, S., & Lam, N. (2004, 2004). *Shear wave velocity profiling in Melbourne silurian mudstone using the spac method.* Paper presented at the Australian Earthquake Engineering Society 2004 Conference, Mt Gambier, SA.

Robinson, D., Fulford, G., & Dhu, T. (2005). EQRM: Geoscience Australia's Earthquake Risk Model. Technical Manual Version 3.0: Record 2005/01: Geoscience Australia: Canberra.

Seckin, M. (1981). *Hysteretic Behaviour of Cast-in-Place Exterior Beam-Column-Slab Subassemblies.* (Ph.D. Thesis), University of Toronto, Toronto, Canada.

Sengupta, P., & Li, B. (2016). Seismic Fragility Assessment of Lightly Reinforced Concrete Structural Walls. *Journal of Earthquake Engineering, 20*(5), 809-840.

Shinozuka, M., Kim, F., Uzawa, T., & Ueda, T. (2001). Statical Analysis of Fragility Curves *Technical Report MCEER*. Department of Civil and Environmental Engineering, University of Southern California.

Sinadinovski, C., McCue, K., & Somerville, M. (2000). Characteristics of strong ground motion for typical Australian intra-plate earthquakes and their relationship with the recommended response spectra. *Soil Dynamics and Earthquake Engineering, 20*(1), 101-110.

Sritharan, S., Beyer, K., Henry, R. S., Chai, Y. H., Kowalsky, M., & Bull, D. (2014). Understanding Poor Seismic Performance of Concrete Walls and Design Implications. *Earthquake Spectra, 30*(1), 307-334. doi:10.1193/021713EQS036M

Standards Australia. (1975). AS 1170.2-1975: Wind Loads (known as the SAA Loading Code Part 2).

Standards Australia. (1979). AS 2121-1979: The design of earthquake-resistant buildings (known as the SAA Earthquake Code).

Standards Australia. (1983). AS 1170.2-1983: Minimum design loads on structures (known as the SAA Loading Code) - Wind loads.

Standards Australia. (1993). AS 1170.4-1993: Minimum design loads on structures (known as the SAA Loading Code) - Earthquake loads.

Standards Australia. (2002). AS 1170.2-2002: Structural design actions, Part 2: Wind Actions.

Standards Australia. (2007). AS 1170.4-2007: Structural design actions, Part 4: Earthquake actions in Australia.

Standards Australia. (2009). AS 3600-2009: Concrete Structures.

Standards Australia. (2011). AS 1170.2-2011: Structural design actions, Part 2: Wind Actions.

Surana, M., Singh, Y., & Lang, D. H. (2015). Seismic Performance of Shear-Wall and Shear-Wall Core Buildings Designed for Indian Codes. In V. Matsagar (Ed.), *Advances in Structural Engineering: Dynamics, Volume Two* (pp. 1229-1241). New Delhi: Springer India.

Tsang, H. H., Menegon, S. J., Lumantarna, E., Lam, N. T. K., Wilson, J. L., Gad, E. F., & Goldsworthy, H. (2016). *Framework for Seismic Vulnerability Assessment of Reinforced Concrete Buildings in Australia*. Paper presented at the Australian Earthquake Engineering Society 2016 Conference, Melbourne, VIC.

Wallace, J. W., Massone, L. M., Bonelli, P., Dragovich, J., Lagos, R., Lüders, C., & Moehle, J. (2012). Damage and Implications for Seismic Design of RC Structural Wall Buildings. *Earthquake Spectra, 28*(S1), S281-S299. doi:doi:10.1193/1.4000047

Walling, M., Silva, W., & Abrahamson, N. (2008). Nonlinear Site Amplification Factors for Constraining the NGA Models. *Earthquake Spectra, 24*(1), 243-255.

Wills, C. J., Petersen, M., Bryant, W. A., Reichle, M., Saucedo, G. J., Tan, S., . . . Treiman, J. (2000). A Site-Conditions Map for California Based on Geology and Shear-Wave Velocity. *Bulletin of the Seismological Society of America, 90*(6B), S187-S208. doi:10.1785/0120000503

Wilson, J., & Lam, N. (2003). A Recommended Earthquake Response Spectrum Model for Australia. *Australian Journal of Structural Engineering, 5*(1), 10.

Wong, P., Vecchio, F., & Trommels, H. (2013). Vector2 and FormWorks User Manual. Department of Civil Engineering, University of Toronto.

Woodside, J. W. (1992). *The new earthquake loading code AS 1170.4*. Paper presented at the Australian Earthquake Engineering Society 1992 Conference, Sydney, Australia.